IFAC Conference on Advances in PID Control
PID'12
Brescia (Italy), March 28-30, 2012 WeB1.4

Oscillation shaping in uncertain linear plants with nonlinear PI control: analysis and experimental results

Alessandro Pilloni Alessandro Pisano and Elio Usai *

* *Dept. of Electrical and Electronic Engineering (DIEE), University of Cagliari, Cagliari, Italy (e–mail: {alessandro.pilloni,pisano,eusai}@diee.unica.it).*

Abstract: Linear systems controlled by a nonlinear version of the PI algorithm are under study. The modified PI controller in question is known in the literature as the Super–Twisting (STW) algorithm (see Levant (1993)), and it belongs to the family of second order sliding mode controllers. The considered closed–loop system exhibits self–sustained stable oscillations (chattering) when the relative degree of the linear plant is higher than one (see Boiko and Fridman (2005)) and it is the task of the present paper to present a systematic yet simple procedure for tuning the STW algorithm parameters in order to obtain pre–specified frequency and magnitude of the resulting chattering oscillation. The proposed methodology is based on the Describing Function (DF) approach. The approach is theoretically illustrated and verified by means of, both, simulation analysis and experiments carried out by making references to a DC motor.

Keywords: Second order sliding modes, Super–Twisting algorithm, Frequency analysis, Chattering adjustment, Nonlinear PI control.

1. INTRODUCTION

PI controllers are widely used in many industrial control systems mainly due to their simplicity, effectiveness and transparency of implementation. Nevertheless, the resulting performance can be unsatisfactory in the presence of strong nonlinearities and/or when non–constant set–point/disturbance need to be tracked/rejected. To overcome these limitations without loosing in simplicity of implementation, a synergic use of PI and sliding mode control (SMC) may be appropriate.

The main drawbacks of classical relay–based SMC (also called "first–order" SMC, or 1–SMC) are principally related to the so–called chattering effect (Utkin et al. (1999)), i.e. undesired high–frequency steady–state vibrations affecting the variables of the plant. To mitigate the chattering effect, a possible solution is the use of higher–order sliding mode control algorithms (HOSM) (Bartolini et al. (1998); Levant (2003)), a set of advanced algorithms that constitute the core of modern SMC theory (Bartolini et al. (2008)).

In this paper we focus our attention on one of the most popular second order sliding mode algorithms known as Super–Twisting algorithm (STW) (Levant (1993)). Among the reasons for the popularity of the STW algorithm, its similarity with the conventional PI, and the fact that it gives rise to a continuous control law, are worth to mention. Whenever applied to linear plants with relative greater than one, STW controlled systems always exhibit chattering (Boiko and Fridman (2005)) in the form of periodic oscillations of the output variable.
We propose in this paper a procedure for selecting the algorithm parameters in order to assign prescribed values to the frequency and amplitude of chattering. The ability to affect the frequency of the residual steady state oscillations may be useful, for example, to mitigate resonant behaviours.

In the literature there are two main approaches to chattering analysis that provide an exact solution in terms of magnitude and frequency of the periodic oscillation:

- time–domain analysis by Poincare Maps (see Gonçalves et al. (2001));
- frequency domain techniques as Tsypikin Locus (see Tsypkin (1984)), and LPRS Method (see Boiko (2009)).

All these approaches require lengthy computations. Therefore, the application of approximate analysis methods has been found useful whenever the plant under analysis fulfill the filtering hypothesis (Atherton (1975)). Under this hypothesis, the Described Function (DF) method is a well–established approach. In fact it has already been used to analyze periodic motions for both 1–SMC (Shtessel and Lee (1996)) and second order SMC (2–SMC) systems (Boiko and Fridman (2005); Boiko et al. (2004, 2006)), and the results obtained via the use of exact techniques often feature a satisfactory similarity with those obtained via the approximate DF method (Boiko (2003)).

In this paper DF–based tools of analysis are exploited for design purposes in the frequency domain in order to provide effective tuning rules for chattering adjustment in linear plants controlled by the STW algorithm.

This paper is organized as follows sections: Section 2 and 3 present the STW algorithm and recall its DF–Based analysis (Boiko and Fridman (2005)). Section 4 states the problem under investigation and presents the tuning procedure for setting the parameters of the STW algorithm in order to assign prescribed amplitude and frequency to the periodic chattering motion. In Sections 5 and 6 the proposed tuning procedure is verified by means of simulations and experimental tests. Section 7 provides some concluding remarks and hints for next research.

2. CONVENTIONAL AND NONLINEAR PI CONTROL FOR LTI PLANTS

Conventional Proportional–Integral (PI) controllers are undoubtedly the most employed controllers in industry. Main advantages of classical PIs are their simplicity, satisfactory performance for "slow" processes, and the availability of effective automatic tuning rules, such as the Ziegler–Nichols or Astrom–Hagglund methods (Astrom and Hagglund (2005)). Internal model principle establishes their capability of providing the asymptotic rejection of constant disturbances and zero steady–state error for constant set–point signals. However, PI controllers may behave unsatisfactorily in presence of strong nonlinearity effects (i.e. friction, hysteresis, backlash) and/or rapidly varying set–point and disturbance signals.

Here we shall investigate linear systems controlled by means of a feedback algorithm which implements a nonlinear version of a PI. The considered controller is known as "Super–Twisting" (STW) Algorithm (see Levant (1993)) and it is described as follows

$$u(t) = u_1(t) + u_2(t) \quad , \tag{1}$$

$$\dot{u}_1 = -\gamma \ \mathrm{sign}\,(\sigma) \quad , \quad u_1\,(0) = 0 \quad , \tag{2}$$

$$u_2 = -\lambda \ \mid \sigma \mid^{\frac{1}{2}} \mathrm{sign}\,(\sigma) \quad , \tag{3}$$

where λ, γ are positive design parameters. It belongs to the family of, so–called, *Second Order Sliding Mode* controllers. A block scheme representing its structure is depicted in Fig. 1. The similarity between the classical PI controller and the nonlinear PI (1)–(3) is evident (see Fig. 2) in that they both possess a static component (a constant proportional gain, for the PI, and a nonlinear gain with infinite slope at the origin for the nonlinear PI) and an integral action (error integration for the PI, and integration of the sign of the error variable for the nonlinear PI).

The STW controller gives rise to a continuous *non–smooth* control action which possesses significant robustness properties against nonlinearities, uncertainties and disturbances. In recent years it has became the most studied SMC algorithm and it has been applied to address control, estimation and fault detection tasks for some classes of linear and nonlinear processes (see Fridman et al. (2007, 2008)).

Whenever applied to systems (possibly nonlinear) having relative degree one, the STW algorithm provides:

- rejection of smooth disturbances of arbitrary shape;
- tracking of smooth references of arbitrary shape;
- finite–time convergence to the set–point.

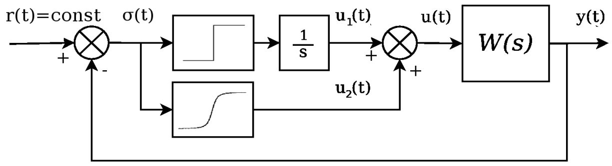

Fig. 1. Block diagram of a linear plant with the Super–Twisting Algorithm.

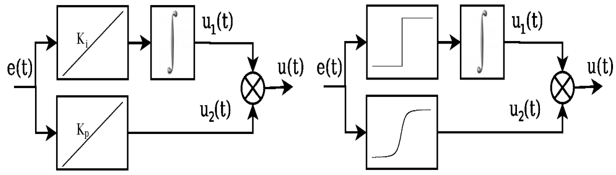

Fig. 2. Architecture Comparison between linear (left) and nonlinear PI.

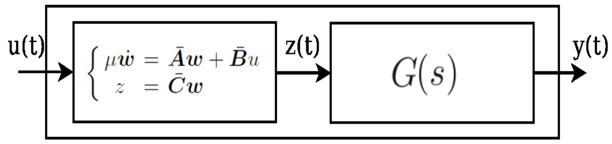

Fig. 3. Decomposition of the arbitrary relative degree plant $W(s)$.

Although the STW algorithm guarantees the finite–time exact convergence for a rather limited class of plants having input–output relative degree one, it was proved its "practical stability" for a wider class of arbitrary relative degree systems admitting a certain decomposition (see Levant and Fridman (2010)). In particular, the following theorem holds once the considered dynamics is formed by the cascade of a stable actuator, of arbitrary relative degree, and a relative degree one dynamics.

Theorem 1. Consider a LTI plant $W(s) = Y(s)/U(s)$, admitting the decomposition shown in Fig. 3, where $H(s) = Z(s)/U(s)$ is an asymptotically stable dynamics with arbitrary relative degree, with the positive coefficient μ scaling its poles as an equivalent time constant, and $G(s)$ is of relative degree one. Then, the feedback control system in Fig. 1 provides the following steady–state condition

$$|\sigma| < O(\mu^2) \quad . \tag{4}$$

■

Theorem 1 follows from (Levant and Fridman (2010)), Lemma 1. The motion within the $O(\mu^2)$ boundary layer (4), established in Theorem 1, proves to be periodic, thereby amenable to be investigated by means of the DF concept (see, e.g. Atherton (1975)).

3. SUPER–TWISTING ALGORITHM AND ITS DF ANALYSIS

We consider a linear SISO system, described by the following state–space representation which comprises principal and parasitic dynamics:

$$\begin{cases} \dot{\boldsymbol{x}}(t) = \boldsymbol{A}\boldsymbol{x}(t) + \boldsymbol{B}u(t), & \boldsymbol{x} \in R^n, \ u \in R \\ y(t) = \boldsymbol{C}\boldsymbol{x}(t), & y \in R \end{cases} \quad , \tag{5}$$

where $\boldsymbol{A}$, $\boldsymbol{B}$, $\boldsymbol{C}$ are matrices of appropriate dimensions, $\boldsymbol{x}$ is the state vector, u is the actuator input, and y the plant output. We shall use the plant description in the form of transfer function as follows

$$W(s) = \frac{Y(s)}{U(s)} = \boldsymbol{C}\,(s\boldsymbol{I} - \boldsymbol{A})^{-1}\,\boldsymbol{B} \quad . \tag{6}$$

We assume that the plant transfer function satisfies the filtering hypothesis property. Using the STW algorithm (1)–(3), the control system under analysis can be represented in the form of the block diagram in Fig. 1 where $\sigma(t) = r(t) - y(t)$ is the error variable. The DF of the nonlinear function (3) was derived in (Boiko and Fridman (2005)) as follows:

$$N_2\,(a_y) = \frac{2\lambda}{\pi\sqrt{a_y}} \int_0^{\pi} (\sin\psi)^{\frac{3}{2}} d\psi = \frac{2\lambda}{\sqrt{\pi a_y}} \frac{\Gamma\,(1.25)}{\Gamma\,(1.75)} \approx 1.1128 \frac{\lambda}{\sqrt{a_y}} \quad , \tag{7}$$

where a_y is the oscillation amplitude of the error variable σ, to be determined, and $\Gamma(\cdot)$ is the Euler's Gamma function. The DF of the nonlinear integral component (2) can be written as follows:

$$N_1\,(a_y, \omega) = \frac{4\gamma}{\pi a_y} \frac{1}{j\omega} \quad , \tag{8}$$

which is the cascade connection of an ideal relay (with the DF equal to $4\gamma/\pi a_y$ (see Atherton (1975))), and an integrator with the frequency response $1/j\omega$. Taking into account both control components in (1), the DF of the STW algorithm (1)–(3) can be finally written as

$$\begin{aligned} N\,(a_y, \omega) &= N_1\,(a_y, \omega) + N_2\,(a_y) \\ &= \frac{4\gamma}{\pi a_y} \frac{1}{j\omega} + 1.1128 \frac{\lambda}{\sqrt{a_y}} \quad . \end{aligned} \tag{9}$$

Let us note that the DF of the STW algorithm depends on, both, the amplitude a_y and frequency ω of the periodic solution.

In general, the parameters of the periodic limit cycle can be approximately found via the solution of the following complex equation

$$1 + W\,(j\omega) \cdot N\,(a_y, \omega) = 0 \quad , \tag{10}$$

so–called, *harmonic balance* (Atherton (1975)). The harmonic balance equation (10) can be rewritten as

$$W\,(j\omega) = -N^{-1}\,(a_y, \omega) \quad , \tag{11}$$

and a periodic oscillation of frequency Ω and amplitude A_y exists when an intersection between the Nyquist plot of the plant $W(j\omega)$ and the negative reciprocal DF $N^{-1}(A_y, \omega)$ occurs at $\omega = \Omega$. Thus, the parameters of the limit cycle can be found via solution of (10) where the DF is given by (9). The negative reciprocal of the DF (9) can be written in explicit form as

$$-\frac{1}{N} = -\frac{0.8986\frac{\sqrt{a_y}}{\lambda} + j1.0282\frac{\gamma}{\omega\lambda^2}}{1 + \frac{1.3091}{a_y}\left(\frac{\gamma}{\omega\lambda}\right)^2} \quad . \tag{12}$$

It is of interest to plot the negative reciprocal of the DF (12) in the complex plane. It depends on the two variables a_y and ω; which are both nonnegative by construction. It is clear from (12) that with positive gains λ and γ the locus is entirely contained in the lower–left quadrant of the complex plane when the variables a_y and ω vary from zero to infinity. In Fig. 4, the curves obtained for $\lambda = 0.6$ and $\gamma = 0.8$, some values $\omega = \omega_i$, and by letting a_y to vary from 0 to ∞ are displayed.

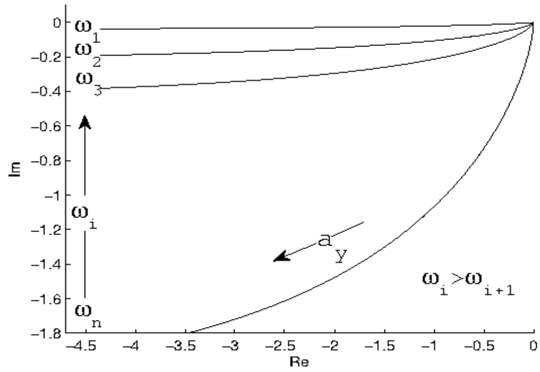

Fig. 4. Plots of the negative reciprocal DF (12) for different values of ω.

3.1 Existence of the Periodic Solution

The harmonic balance (10) can be also expressed as

$$N\,(A_y, \Omega) = W^{-1}(j\Omega) \quad , \tag{13}$$

which, considering (9), specializes to

$$\frac{4\gamma}{\pi A_y} \frac{1}{j\Omega} + 1.1128 \frac{\lambda}{\sqrt{A_y}} = -W^{-1}(j\Omega) \quad . \tag{14}$$

Separating the complex equation (14) in its real and imaginary parts it yields

$$\begin{cases} 1.1128 \dfrac{\lambda}{\sqrt{A_y}} = -\operatorname{Re} W^{-1}(j\Omega) \\ \dfrac{4\gamma}{\pi\Omega} \dfrac{1}{A_y} = \operatorname{Im} W^{-1}(j\Omega) \end{cases} \quad . \tag{15}$$

Obtaining A_y from the first of (15) and substituting this value in the second equation of (15), it yields

$$\frac{4\gamma}{\pi\Omega} \frac{1}{\operatorname{Im} W^{-1}(j\Omega)} - \left(\frac{1.1128\lambda}{-\operatorname{Re} W^{-1}(j\Omega)}\right)^2 = 0 \quad , \tag{16}$$

which allows to compute the frequency Ω. Solution of (16) cannot be derived in closed form, and a numerical, or graphical, approach is mandatory.

Once obtained Ω , the amplitude of the periodic solution can be expressed as

$$A_y = \frac{4\gamma}{\pi\Omega} \frac{1}{\operatorname{Im} W^{-1}(j\Omega)} \quad . \tag{17}$$

As noticed in (Boiko and Fridman (2005)), a point of intersection between the Nyquist plot of the plant and the negative reciprocal of the STW DF (9) always exists if the relative degree of the plant transfer function is higher than one, and this point is located in the third quadrant of the complex plane. From Fig. 4, it is also apparent that the frequency of the periodic solution induced by the STW is always lower than the frequency of the periodic motion for the system controlled by the conventional relay.

The orbital asymptotic stability of the periodic solution can be assessed using the *Loeb Criterion* (see Atherton (1975); Gelb and Vander Velde (1968)), that is not mentioned here for the sake of brevity.

4. PROBLEM FORMULATION AND PROPOSED TUNING PROCEDURE

4.1 Problem Formulation

Consider the feedback control system in Fig. 1, where the plant is modelled by an unknown transfer function $W(s)$ having relative degree greater than one. Given the steady–state performance requirements in terms of desired frequency Ω_d and amplitude A_{y_d} of the chattering motion, we aim to define a tuning procedure, based on the DF method, devoted to derive constructive controller tuning rules for the algorithm (1)–(3).

To begin with, let us substitute (12) into (11) and rewrite the harmonic balance equation as

$$W(j\omega) = -\frac{c_1 \frac{a_y^{1.5}}{\lambda}}{a_y + c_3\left(\frac{\gamma}{\omega\lambda}\right)^2} - j\frac{c_2 \frac{a_y \gamma}{\omega\lambda^2}}{a_y + c_3\left(\frac{\gamma}{\omega\lambda}\right)^2} \quad , \tag{18}$$

with $c_1 = 0.8986$, $c_2 = 1.0282$, $c_3 = 1.3091$. Let

$$K_1(\omega) = \frac{\gamma}{\omega} \quad , \quad K_2(\omega) = \frac{\gamma}{\omega\lambda} \quad . \tag{19}$$

Multiplying both sides of (18) by γ/ω, we derive

$$K_1(\omega) W(j\omega) = -\frac{c_1 a_y^{1.5} K_2(\omega)}{a_y + c_3 K_2^2(\omega)} - j\frac{c_2 a_y K_2^2(\omega)}{a_y + c_3 K_2^2(\omega)} \quad . \tag{20}$$

Once considered the design requirements $a_y = A_{y_d}$ and $\omega = \Omega_d$, separating the complex equation (20) in its magnitude and phase as follows

$$K_1(\Omega_d)\left|W(j\Omega_d)\right| = \sqrt{\frac{c_1^2 A_{y_d}^3 K_2(\Omega_d) + c_2^2 A_{y_d}^2 K_2(\Omega_d)}{\left(A_{y_d} + c_3 K_2^2(\Omega_d)\right)^2}} \tag{21}$$

$$\arg\left\{W(j\Omega_d)\right\} = \operatorname{atan}\left\{\frac{c_2 K_2(\Omega_d)}{c_1\sqrt{A_{y_d}}}\right\} \tag{22}$$

we obtain a well–posed system of equations, where $K_1^d = K_1(\Omega_d)$ and $K_2^d = K_2(\Omega_d)$ are the two unknowns. The magnitude and phase of $W(j\omega)$ at the desired chattering frequency Ω_d can be identified by a simple test on the plant. Therefore, solving (21)–(22), and then considering (19) with $\omega = \Omega_d$, we derive the controller parameters λ and γ that guarantee a steady–state periodic motion with desired characteristics. Corresponding formulas are

$$\begin{cases} \gamma = \Omega_d K_1^d \\ \lambda = \dfrac{\gamma}{\Omega_d K_2^d} = \dfrac{K_1^d}{K_2^d} \end{cases} \tag{23}$$

Direct solution of the nonlinear equations (21)–(22) can be avoided. By following a graphical approach it is convenient to refer to the curves in Fig. 5, where each curve represents a specific instance of the right–hand side of (20) in the complex plane, for different values of A_{y_d}, by letting K_2 to vary from 0 to ∞. Drawing in the abacus a segment connecting the origin of the complex plane and the point P of the curve associated to A_{y_d}, with phase equal to $\arg\{W(j\Omega_d)\}$ (see Fig. 10), we can extrapolate the length of the segment $\overline{OP}$ which corresponds to the right–hand side of (21). Then, once known $\overline{OP}$, we can compute K_1^d and K_2^d by the following relationship

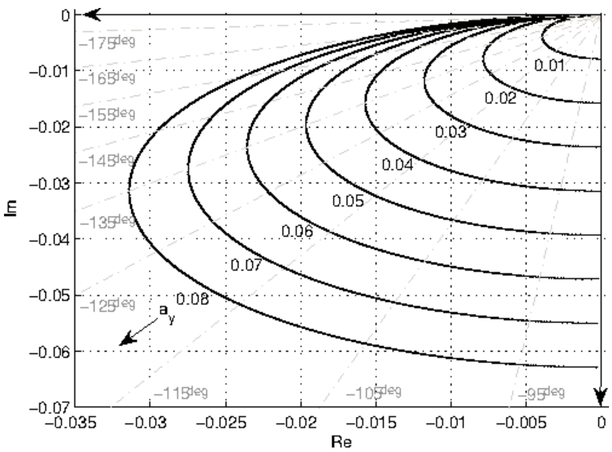

Fig. 5. Level sets of the right–hand of (20) for different values of a_y and $K_2 \in (0, \infty)$.

$$\begin{cases} K_1^d = \dfrac{\overline{OP}}{\left|W(j\Omega_d)\right|} \\ K_2^d = \dfrac{c_1\sqrt{A_{y_d}}}{c_2}\tan\left\{\arg\left\{W(j\Omega_d)\right\}\right\} \end{cases} \tag{24}$$

Remark 1. It is important to underline that the intersection between the Nyquist plot of $W(j\omega)$ and $-N^{-1}(a_y, \omega)$ always lies in the lower–left quadrant of the complex plane, so the desired frequency of chattering oscillation Ω_d must satisfy the sector condition

$$\Omega_1 < \Omega_d < \Omega_2 \tag{25}$$

where

$$\arg\left\{W(j\Omega_1)\right\} = \frac{\pi}{2} \quad , \quad \arg\left\{W(j\Omega_2)\right\} = \pi \tag{26}$$

■

Remark 2. The right–hand side of (20) is independent of the plant transfer function. Therefore the set of curves in Fig. 5 represents an *abacus*, independent of the plant, too, hence very useful to simplify the solution of (20).

■

4.2 Proposed Tuning Procedure

Given a *low–pass plant with relative degree greater than one*, we can summarize the proposed procedure:

Procedure 1.

A. Let A_{y_d} and Ω_d be the desired chattering characteristics;
B. Evaluate by an harmonic response test on the plant the quantities $|W(j\Omega_d)|$ and $\arg\{W(j\Omega_d)\}$ and check if $\pi/2 < \arg\{W(j\Omega_d)\} < \pi$, otherwise chose a different value for Ω_d and go back to step A;
C. Draw in the abacus a segment connecting the origin and the point P of the curve $a_y = A_{y_d}$ with phase equal to $\arg\{W(j\Omega_d)\}$;
D. Use (23) to compute λ and γ.

5. SIMULATION RESULTS

In order to outline the proposed methodology, we consider the cascade connection of a linear plant $G(s)$ and a stable

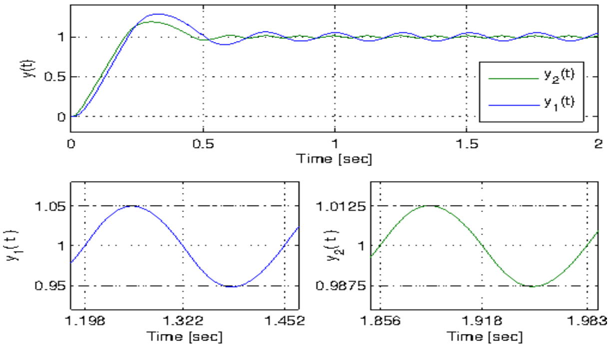

Fig. 6. Step response of the plant $W(s)$ in closed–loop with STW parameters $\lambda = 5.0119$, $\gamma = 18.3575$.

actuator $H(s)$, such that the relative degree of $W(s) = H(s) \cdot G(s)$ is greater than one, i.e.:

$$G(s) = \frac{s+1}{s^2+s+1} \quad , \quad H(s) = \frac{1}{(\mu s+1)^2} \quad , \tag{27}$$

$$W(s) = H(s) \cdot G(s) \quad , \quad \mu = 1/50 \quad .$$

Let us apply Procedure 1 to shape the steady–state permanent oscillation of the closed–loop system with the STW algorithm.

A. Let $A_{y_d} = 0.05$ and $\Omega_d = 25$ rad/sec;
B. By frequency response test we obtain:
$$|W(j\Omega_d)| \approx 0.032 \quad , \quad \arg\{W(j\Omega_d)\} \approx -143.14 \text{ deg} \quad ;$$
C. Drawing the segment $\overline{OP}$ in the abacus until it intersects the curve associated to a_{y_d} (see Fig. 10), we derive
$$\overline{OP} = \sqrt{(-0.01882)^2 + (-0.01414)^2} = 0.0235 \quad ;$$
D. Using (24) and (19) obtain
$$\lambda = 5.0119 \quad , \quad \gamma = 18.3575 \quad . \tag{28}$$

In Fig. 6, some simulation results are shown. Signal $y_1(t)$ represents the closed–loop unit–step response of the plant (27) with control parameters (28). Signal $y_2(t)$ represent the output signal obtained using the reduced value $\mu = 1/100$ for the actuator time constant parameter. The bottom left zoomed sub–plot confirms that the steady–state chattering motion fulfills the given specification of amplitude and frequency. The bottom right sub–plot shows that the chattering amplitude a_y is 4 times smaller, according to Theorem 1. The achieved results fully agree with the presented analysis.

6. EXPERIMENTAL RESULTS

The proposed method has been experimentally tested with reference to the position control of a commercial DC Motor. In Fig. 7 the experimental setup is shown.

As first step (Step A), the desidered frequency and magnitude of the periodic oscillation were set as

$$A_{y_d} = 0.05 \quad , \quad \Omega_d = 50 \text{ rad/sec} \quad . \tag{29}$$

Then, by an harmonic test (Step B), we have obtained the values

$$|W(j\Omega_d)| \approx 0.0081 \quad , \quad \arg\{W(j\Omega_d)\} \approx -138.7 \text{ deg} \quad . \tag{30}$$

Afterwards, by the abacus in Fig. 5 (Step C) we calculate

$$\overline{OP} = \sqrt{(-0.0195)^2 + (-0.0171)^2} = 0.0259 \tag{31}$$

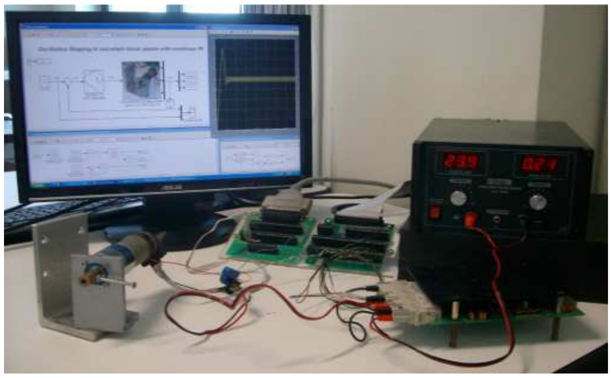

Fig. 7. Experimental set–up with FAULHABER® DC Micromotor Series 3557 024 CS.

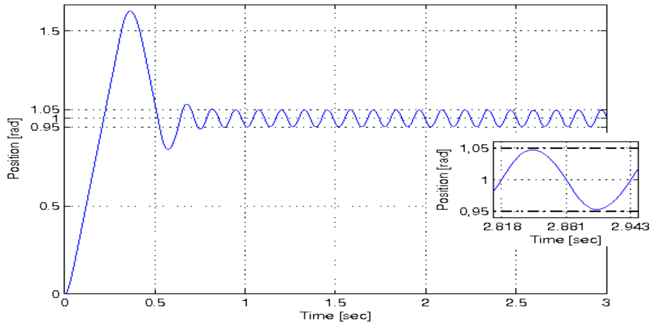

Fig. 8. Experimental step response of the DC–Motor in closed–loop with $\lambda = 18.64$, $\gamma = 159.99$.

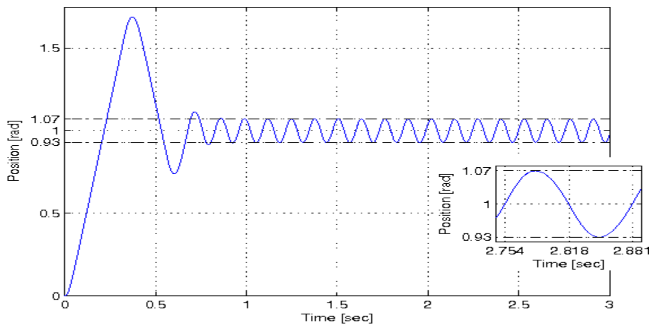

Fig. 9. Experimental step response of the DC–Motor in closed–loop with $\lambda = 20.05$, $\gamma = 223.99$.

from which, (Step D) we obtain the designed gains for the nonlinear PI (1)–(3)

$$\lambda = 18.64 \quad , \quad \gamma = 159.99 \quad . \tag{32}$$

In Fig. 8, the closed–loop unit–step response of the motor with control parameters (32) is displayed. It can be checked that the actual amplitude and frequency of the oscillation closely match the desired ones. A second experiment has been made by evaluating the parameters giving rise to a periodic oscillations having the same frequency $\Omega_d = 50$ rad/sec and a different, bigger, amplitude $A_{y_d} = 0.07$. By repeating the suggested tuning procedure, the next controller parameters were obtained

$$\lambda = 20.05 \quad , \quad \gamma = 223.99 \quad . \tag{33}$$

The results of the corresponding experiment are shown in the Fig. 9, which shows, again, an almost perfect matching between the actual and expected characteristics of the steady state oscillation.

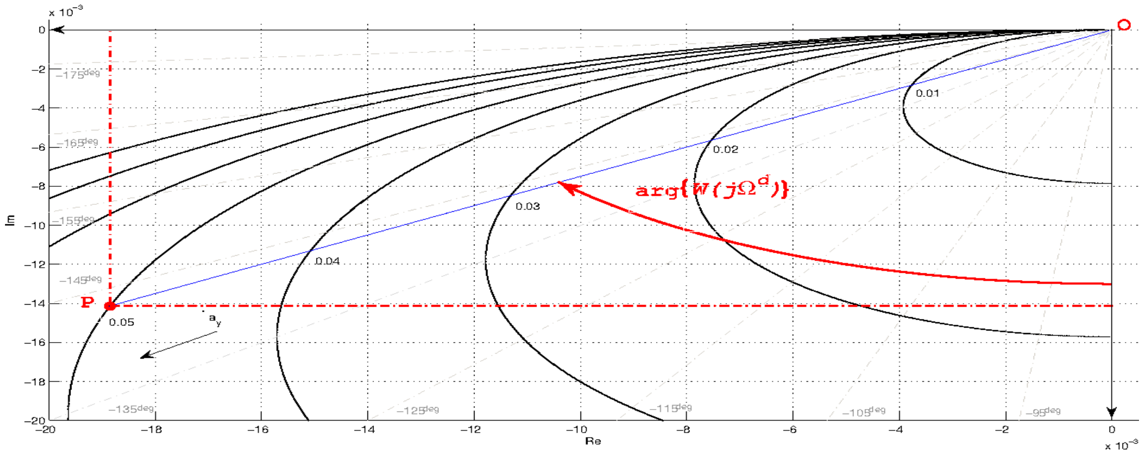

Fig. 10. Example of abacus utilization for the system $W(s)$ (27).

7. CONCLUSIONS AND FUTURE WORKS

A describing function approach to controller tuning has been presented, to be adopted for linear SISO plants driven by a nonlinear PI controller. The main property of the suggested tuning procedure is that it allows to set a–priori the amplitude and the frequency of the self–sustained steady state periodic oscillations that take place in this class of system when the relative degree is higher than one. The proposed procedure has been tested by means of computer simulations and experiments. Among some interesting directions for improving the present result, the analysis, and shaping, of the transient oscillations is of special interest to avoid possibly large transient overshoots. The mathematical treatment presented in Boiko (2011) and the “dynamic harmonic balance” could be a starting point for generalizing the present procedure along that direction. Additionally, strategies for the on–line adjustment of the controller parameters could be devised within the present line of investigation to achieve satisfactory transient and steady state performance at the same time.

REFERENCES

Astrom, K. and Hagglund, T. (2005). *Advanced PID Control*. ISA - The Instrumentation, Systems, and Automation Society. Research Triangle Park, NC 27709,

Atherton, D. (1975). *Nonlinear Control Engineering–Describing Function Analysis and Design*. Workingham Berks, U.K.

Bartolini, G., Ferrara, A., and Usai, E. (1998). Chattering avoidance by second–order sliding mode control. *IEEE Trans. Aut. Contr.*, 43(2), 241–246.

Bartolini, G., Fridman, L., Pisano, A., and Usai, E., (Eds) (2008). Modern Sliding Mode Control Theory. New Perspectives and Applications. *Springer Lecture Notes in Control and Information Sciences*, Vol. 375.

Boiko, I. (2003). Analysis of sliding mode control systems in the frequency domain. In *Proc. of the 2003 American Control Conference (ACC 2003)*, volume 1, 186–191.

Boiko, I. (2009). *Discontinuous control systems: frequency–domain analysis and design*. Boston, Birkhauser, 2009.

Boiko, I. Dynamic harmonic balance and its application to analysis of convergence of second–order sliding mode control algorithms. In *Proc. of the 2011 American Control Conference (ACC 2011)*, volume 1, 208–213.

Boiko, I. and Fridman, L. (2005). Analysis of chattering in continuous sliding–mode controllers. *IEEE Trans. Aut. Contr.*, 50(9), 1442–1446.

Boiko, I., Fridman, L., and Castellanos, M. (2004). Analysis of second–order sliding–mode algorithms in the frequency domain. *IEEE Trans. Aut. Contr.*, 49(6), 946–950.

Boiko, I., Fridman, L., Iriarte, R., Pisano, A., and Usai, E. (2006). Parameter tuning of second–order sliding mode controllers for linear plants with dynamic actuators. *Automatica*, 42(5), 833–839.

Burton, J. (1986). Continuous approximation of variable structure control. *Int. J. of Systems Science*, 17(6), 875–886. Taylor and Francis.

Fridman, L., Davila, J., and Levant, A. (2007). High–order sliding–mode observation and fault detection. In *Proc. of the 2007 IEEE Conference on Decision and Control (CDC 2007)*, 43174322.

Fridman, L., Shtessel, Y., Edwards, C., and Yan, X. (2008). Higher–order sliding–mode observer for state estimation and input reconstruction in nonlinear systems. *Int. J. of Robust and Nonlinear Control*, 18(4–5), 399–412.

Gelb, A. and Vander Velde, W. (1968). *Multiple–input describing functions and nonlinear system design*. McGraw–Hill, New York.

Gonçalves, J., Megretski, A., and Dahleh, M. (2001). Global stability of relay feedback systems. *IEEE Trans. Aut. Contr.*, 46(4), 550–562.

Levant, A. (1993). Sliding order and sliding accuracy in sliding mode control. *Int. J. of Control*, 58(6), 1247–1263.

Levant, A. (2003). Higher–order sliding modes, differentiation and output–feedback control. *Int. J. of Control, 76*, 9(10), 924–941.

Levant, A. and Fridman, L. (2010). Accuracy of homogeneous sliding modes in the presence of fast actuators. *IEEE Trans. Aut. Contr.*, 55(3), 810–814.

Shtessel, Y. and Lee, Y. (1996). New approach to chattering analysis in systems with sliding modes. In *Proc. of the 1996 IEEE Conference on Decision and Control (CDC 1996)*, volume 4, 4014–4019.

Tsypkin, Y.Z. (1984). *Relay control systems*. Cambridge University Press.

Utkin, V., Guldner, J., and J., S. (1999). *Sliding mode control in electromechanical systems*. Taylor and Francis, London, 1999.